Adv Healthc Mater. Author manuscript; available in PMC 2017 November 01.

Published in final edited form as:

Adv Healthc Mater. 2016 November ; 5(21): 2745–2750. doi:10.1002/adhm.201600599.

Mucus-penetrating Nanosuspensions for Enhanced Delivery of Poorly Soluble Drugs to Mucosal Surfaces

Tao Yu,

Center for Nanomedicine, The Wilmer Eye Institute, Johns Hopkins University School of Medicine, 400 N Broadway, Baltimore, MD 21231 (USA). Department of Biomedical Engineering, Johns Hopkins University School of Medicine, 720 Rutland Avenue, Baltimore, MD 21205 (USA)

Woo-Jin Choi,

Department of Biomedical Engineering, Johns Hopkins University School of Medicine, 720 Rutland Avenue, Baltimore, MD 21205 (USA)

Abraham Anonuevo,

Department of Chemical and Biomolecular Engineering, Johns Hopkins University, 3400 N Charles Street, Baltimore, MD 21218 (USA)

Jane Chisholm,

Center for Nanomedicine, The Wilmer Eye Institute, Johns Hopkins University School of Medicine, 400 N Broadway, Baltimore, MD 21231 (USA). Department of Chemical and Biomolecular Engineering, Johns Hopkins University, 3400 N Charles Street, Baltimore, MD 21218 (USA)

Sarah Pulicare,

Department of Chemical and Biomolecular Engineering, Johns Hopkins University, 3400 N Charles Street, Baltimore, MD 21218 (USA)

Weixi Zhong,

Department of Biomedical Engineering, Johns Hopkins University School of Medicine, 720 Rutland Avenue, Baltimore, MD 21205 (USA)

Minmin Chen,

Center for Nanomedicine, The Wilmer Eye Institute, Johns Hopkins University School of Medicine, 400 N Broadway, Baltimore, MD 21231 (USA)

Colleen Fridley,

Department of Chemical and Biomolecular Engineering, Johns Hopkins University, 3400 N Charles Street, Baltimore, MD 21218 (USA)

Prof. Samuel K. Lai,

Eshelman School of Pharmacy, University of North Carolina at Chapel Hill, Campus box 7362, Chapel Hill, NC 27599 (USA)

Correspondence to: Justin Hanes.

Experimental

Detailed experimental methods are provided in Supporting Information.

((Supporting Information is available online from Wiley InterScience or from the author)).

Prof. Laura M. Ensign,
Center for Nanomedicine, The Wilmer Eye Institute, Johns Hopkins University School of Medicine, 400 N Broadway, Baltimore, MD 21231 (USA). Department of Ophthalmology, The Wilmer Eye Institute, Johns Hopkins University School of Medicine, 600 N Wolfe Street, Baltimore, MD 21297 (USA)

Prof. Jung Soo Suk, and
Center for Nanomedicine, The Wilmer Eye Institute, Johns Hopkins University School of Medicine, 400 N Broadway, Baltimore, MD 21231 (USA). Department of Ophthalmology, The Wilmer Eye Institute, Johns Hopkins University School of Medicine, 600 N Wolfe Street, Baltimore, MD 21297 (USA)

Prof. Justin Hanes
Center for Nanomedicine, The Wilmer Eye Institute, Johns Hopkins University School of Medicine, 400 N Broadway, Baltimore, MD 21231 (USA). Department of Biomedical Engineering, Johns Hopkins University School of Medicine, 720 Rutland Avenue, Baltimore, MD 21205 (USA). Department of Chemical and Biomolecular Engineering, Johns Hopkins University, 3400 N Charles Street, Baltimore, MD 21218 (USA). Department of Ophthalmology, The Wilmer Eye Institute, Johns Hopkins University School of Medicine, 600 N Wolfe Street, Baltimore, MD 21297 (USA)

Abstract

Mucus-penetrating Nanosuspensions, consisting of pure hydrophobic therapeutics with dense muco-inert coatings that enable particles to effectively bypass the mucus barrier, demonstrate superior drug distribution and absorption at mucosal surfaces. With significantly increased drug load compared to polymeric systems and established clinical translation of nanosuspensions-based products, mucus-penetrating nanosuspensions are a promising vehicle for improving mucosal delivery of poorly soluble drugs.

Keywords

nanocrystal; drug delivery; mucus penetrating particles; nanotechnology; curcumin

---

Delivery systems that can more effectively deliver drugs to mucosal surfaces are needed.[1] For efficient delivery to mucosal surfaces, drugs and drug carriers have to first bypass the adhesive mucus gel, a barrier that has evolved to protect the underlying tissues by efficiently trapping and removing foreign pathogens or particles.[2] Mucus is a mesh that traps particulates both sterically and adhesively, thus size and surface characteristics play a significant role.[3] It was reported that nanoparticles with sizes smaller than the mucus mesh and densely coated with a muco-inert material (poly(ethylene glycol), or PEG), can rapidly diffuse through human mucus secretions.[4] These “mucus-penetrating particles (MPP)”, have demonstrated improved mucosal distribution, enhanced pharmacokinetics, and superior treatment efficacy in applications such as prevention of genital herpes infection,[5] treatment of cervical cancer,[6] and lung gene therapy.[7] Nanosuspensions (NS), which are nano-sized particulates fabricated from insoluble drug precipitates and stabilized with surface coatings, have become a widely used dosage form in pharmaceutical applications.[8] While prior MPP systems have largely been based on biodegradable polymers and, thus, usually contain 20% drug or less by weight, NS formulated based on pure, water insoluble drugs can achieve higher drug content, a feature that is critical for delivery to mucosal regions with highly limited dosing volume/mass, such as the nasal and sinus cavities and the eyes.[9] Furthermore, the increased surface-to-volume ratio in NS facilitates the dissolution of the drugs, especially those otherwise hardly soluble under physiological conditions.[8;10] NS may thus be suitable for applications that require fast drug uptake,[11] such as treatment of acute indications, like asthma, or coitally-associated pre-exposure prophylaxis of viral infections, such as HIV. Additionally, the simple composition and well-established manufacturing practices for producing NS have accelerated clinical development, with at least 9 NS-based therapeutic products successfully marketed to date.[12] These favorable features have attracted broad interest in the development of NS formulations, especially for intravenous and oral administration.[12–13] However, the interactions between NS and mucus, as well the development of NS that can penetrate mucus barriers to improve mucosal drug delivery, have yet to be investigated. Here, we report the development of mucus-penetrating NS for efficient delivery of poorly soluble drugs to mucosal surfaces.

We have previously shown that hydrophobic polymeric nanoparticles (~200–300 nm in diameter) with mucoadhesive surface chemistry can be made mucoinert by densely coating the nanoparticle surface with particular Pluronics®.[4b] Pluronics are triblock copolymers composed of a hydrophobic poly(propylene oxide) (PPO) core and two hydrophilic PEG arms. The PPO core of certain Pluronics can adsorb onto hydrophobic nanoparticle surfaces, while the PEG chains, at sufficient density, shield the particle surface from electrostatic and hydrophobic interactions with mucus.[14] We therefore first tested whether coating with Pluronic F127 (abbreviated as F127 hereafter) could reduce the adhesion of similarly sized and hydrophobic NS to mucus. F127 is a Generally Regarded As Safe (GRAS) by the FDA material in multiple pharmaceutical products.[4b;14] We selected curcumin (CUR) as a model drug to formulate NS. CUR has been widely reported as an anti-inflammatory, anti-oxidant, anti-tumor and anti-viral therapeutic.[15] However, the extremely low solubility of CUR in water leads to its poor bioavailability *in vivo*, and thus limits its use; CUR delivered systemically can also be readily metabolized and deactivated in the liver.[16] Local delivery of CUR as a NS formulation may therefore be an ideal approach to address these limitations. In addition, CUR possesses strong and stable fluorescence,[17] which allows the observation of CUR NS in mucus using fluorescence microscopy without the need for complicated labeling and alteration of CUR properties. Due to these properties, various nano-formulations of CUR have been widely investigated, including several that employed Pluronics as stabilizers.[18]

We formulated CUR-F127 NS via high power probe sonication similar to conventional top-down NS formulation approaches.[19] Powder X-ray diffractometry (XRD) confirmed that CUR-F127 NS preserved the crystallinity of unprocessed CUR, as the characteristic peaks of CUR-F127 NS matched those of the raw CUR (Figure 1a). The signature peaks of F127 were not apparent in the XRD profile of CUR-F127 NS, suggesting that the NS were composed mainly of CUR and a small proportion of F127 (Figure 1a). We also measured the fluorescence spectrum of CUR-F127 NS to confirm that the processing did not quench the CUR fluorescence (Figure S1). To further show that the fluorescent signal was indeed emitted from the NS, we imaged the CUR-F127 NS with both fluorescence and bright field microscopy. When merged, the fluorescence signal was co-localized with the particles in the bright field image (Figure S2). Transmission electron microscopy (TEM) showed that the morphology of CUR-F127 NS was relatively irregular, likely due to the randomness of the shearing process during probe sonication (Figure 1b). The mean diameter of CUR-F127 NS was 133 nm (Table 1), consistent with the average size indicated by TEM. The average mesh size of human mucus secretions, including cervicovaginal, airway and sinus mucus, ranges from ~140 to 340 nm, with a wide distribution of mesh sizes.[2a;20] Thus, the small size of CUR-F127 NS was appropriate for diffusion through mucus. The ζ-potential of 210 nm carboxylate-functionalized polystyrene nanoparticles (PS-COOH, previously reported to be strongly mucoadhesive [20–21]) was highly negative (Table 1), and in previous work, a change to near-neutral ζ-potential was indicative of effective PEG surface coating.[4] However, the ζ-potential of CUR-F127 NS was not necessarily indicative of the extent of surface coverage, as the NS were near-neutrally charged regardless of surface coating due to the intrinsic drug properties (Table 1). For this reason, investigation of the NS diffusion in mucus was essential for evaluating the effectiveness of surface coatings at reducing interactions with mucus.

To determine whether formulating the NS with F127 effectively coated the surface of the CUR, we next investigated the transport behavior of CUR-F127 NS in cervicovaginal mucus (CVM) freshly collected from healthy donors. We first viewed the CVM alone (i.e. without the addition of CUR NS) at the same settings to ensure that auto-fluorescence in the sample would not interfere with visualization of the CUR NS (Figure S3a). In contrast, the CUR-F127 NS fluorescence was clearly visible as dispersed particulates in CVM (Figure S3b). CUR-F127 NS exhibited highly diffusive time-lapse trajectories over the course of 20 s movies, suggesting Brownian-like diffusion (Movie S1); in contrast, the mucoadhesive PS-COOH nanoparticles were immobilized, exhibiting highly restricted, non-Brownian traces (Figure 2a). To further quantify the differences in transport rates of CUR-F127 NS and PS-COOH particles in CVM, we measured the ensemble-averaged mean-squared displacement (<MSD>) of the particles as a function of time scale; greater <MSD> represents faster particle movement. The <MSD> of CUR-F127 NS was 4,400-fold higher than that of PS-COOH at a time scale of 1 s (Table 1), and at least two orders of magnitude higher across all time scales analyzed up to 3 s (Figure 2b). The <MSD> of PS-COOH nanoparticles was 25,000-fold lower than the theoretical MSD of similarly sized nanoparticles in water at a time scale of 1 s, whereas the <MSD> of CUR-F127 NS was only 9-fold lower (Table 1). Distributions of the logarithmic MSD (at a time scale of 1 s) of individual particles further demonstrate that the CUR-F127 NS were uniformly diffusive in CVM (Figure 2c). Overall, CUR-F127 NS demonstrated diffusion rates comparable to that of previous polymer-based MPP formulations.[4b–e]

We then characterized the diffusion rates of CUR-F127 NS in airway sputum freshly expectorated by cystic fibrosis (CF) patients (cystic fibrosis sputum; CFS), a critical barrier for inhaled CF therapies. In CF patients, impaired ion transport leads to a more viscoelastic mucus that impairs mucociliary clearance and provides a permissive environment for chronic infection and inflammation, further contributing to the dense mucus mesh structure.[3] Similar to the results in CVM, CUR-F127 NS demonstrated more diffusive trajectories and increased individual MSD as compared to the mucoadhesive PS-COOH particles (Figure 2d–f). At a time scale of 1 s, the mobility of CUR-F127 NS was 37-fold slower than the theoretical speed of similarly sized nanoparticles in water (Table 1), comparable to that of previously reported MPP formulations in CFS. The mobility of CUR-F127 NS in CFS was slightly more constrained than that in CVM, likely due to the smaller mesh size of CFS (average ~ 140 nm, with a range of 60–300 nm [20b]) and respiratory mucus.[20c;20d] While mucus from different anatomical regions may have different structural properties, this and other work suggests that an effective mucoinert surface coating will generally reduce adhesion to various types of mucus secretions.[2a;4e;22] These results suggest that CUR-F127 NS may penetrate mucus at multiple mucosal surfaces, even in diseased states, and therefore may be broadly useful for various applications. In addition, CUR-F127 NS showed dissolution rates over 30-fold faster than that of raw CUR (Figure S4); this enhanced dissolution capability should facilitate the rapid absorption of CUR by target tissues.[23]

To further understand the formulation requirements for muco-inert NS coatings, we examined the mobility in human CVM of CUR NS formulated at different F127 concentrations. While all formulations exhibited sizes below the average mesh spacing of CVM, the size of CUR NS increased as the concentration of F127 decreased, suggesting that F127 exerts a stabilizing effect on the CUR NS during fabrication (Table 1). CUR NS prepared with minimal (0.001%) F127 solution showed significantly reduced mobility in CVM similar to that of PS-COOH particles, reflecting the mucoadhesive nature of the hydrophobic CUR NS core and lack of muco-inert coating. A 10-fold increase of F127 concentration to 0.01% resulted in an over 300-fold increase of the <MSD> of CUR NS in CVM, and further increases in F127 concentrations resulted in incremental increases in the <MSD>. The over 300-fold increase in <MSD> between 0.001% and 0.01% F127 suggested an increase in the adsorption of F127 onto the surface of CUR, providing effective coatings even within this low concentration range. Effective adsorption of F127 is likely critical for maintaining NS stability and the ability of the NS to resist mucoadhesion. The wide range of effective F127 concentrations that provide effective muco-inert coatings may also provide more engineering flexibility for formulation optimization specific to different fabrication methods or applications.[19]

We screened 11 additional Pluronics and 3 other PEG-containing surfactants (i.e., Tween® 20, Tween® 80 and Vitamin E-TPGS) to establish selection criteria for materials that are suitable as muco-inert NS coatings. Many of the CUR NS formulated in the presence of Pluronics demonstrated improved mobility in CVM as compared to the mucoadhesive 200 nm PS-COOH, with notable exceptions (Figure 3 and Table S1). In contrast, the 3 PEG-containing surfactants tested failed to provide sufficient PEG coatings on CUR NS to reduce adhesion in CVM (Table S2). To investigate the underlying phenomenon determining whether the Pluronics formed a sufficient muco-inert coating on the CUR NS, we mapped the <MSD> of CUR-Pluronics NS as a function of the molecular weight (MW) of the Pluronic PPO and PEG segments. As shown in Figure 3, the mobility of CUR-Pluronics NS correlated with the PPO MW (correlation coefficient $r = 0.94$), but was independent of PEG MW ($r=0.12$), with effective shielding achieved at PPO MW above ~ 2.6 kDa regardless of PEG MW (~ 0.7–5.8 kDa). Similarly, the non-Pluronic surfactants containing PEG chains of

MW (~1 kDa) comparable to the Pluronics that effectively coated the CUR NS (e.g. P123), but lower MW hydrophobic segments (~0.3–0.5 kDa), failed to form a sufficient muco-inert coating on the CUR NS (Table S2), further suggesting that the effectiveness of the surface coating is dependent on the affinity of the hydrophobic segments to the NS surface. A high affinity interaction would lead to efficient adsorption of the surfactant onto the NS surface, and thus provide a highly compacted, brush-like PEG surface layer even at PEG MW as low as ~ 750 Da (i.e., P103).[24] These engineering principles provide general guidelines for the selection or design of appropriate surfactants that enable NS, and other hydrophobic carriers as previously suggested,[4b;25] to bypass mucus and potentially other adhesive biological barriers.[26] Although we have demonstrated that surface coating by certain Pluronics is sufficient to reduce adhesive interactions of nanosuspensions with the mucus mesh, it has yet to be studied whether a protein corona forms on the surfaces of Pluronic-coated nanoparticles in mucus.[27] It is not necessarily expected that nanosuspensions will be taken up by cells as intact nanoparticles, but such surface modifications could potentially affect cell uptake and intracellular trafficking of Pluronic-coated nanoparticles that are internalized intact *in vivo*.

We next investigated whether CUR-F127 NS diffusion in mucus would lead to improved mucosal surface distribution *in vivo*. We selected raw CUR and CUR NS coated with F68 (CUR-F68 NS), another Pluronic that is widely used in pharmaceutical products,[4b;14] to compare to the muco-inert CUR-F127 NS. Based on the screening results, F68 was an insufficient coating material for the NS (Movie S2), as the average diffusion rates of F68-CUR NS were ~20-fold slower than CUR-F127 NS in CVM at a time scale of 1 s (Table 1). Moreover, we confirmed that the CUR-F68 NS was not stable when incubated in a model mucin solution, further suggesting that the F68 does not provide a sufficient surface coating to prevent interactions with mucins (Figure S5). In contrast, the average size of the CUR-F127 NS remained relatively constant during 12 h of incubation in mucin solution (Figure S5). Mice were dosed intranasally to examine CUR distribution in the mouse airways. Representative images of transverse sections of the large airways are shown in Figure 4a. These images were used to quantify the uniformity (coefficient of variation, C.V.) and overall coverage of CUR distribution, measured as a percentage of the epithelium with fluorescence above the tissue background (Figure 4b,c). Lower C.V. values and higher percentages of coverage represent improved mucosal drug distribution. Raw CUR were aggregated within the airway lumen and provided limited coverage of the mucosa (C.V. = 2.14 ± 0.12, coverage = 11 ± 3%). Both the large size and hydrophobicity of the raw CUR can lead to trapping in the mucus gel.[4e] While both the F68- and F127-containing NS formulations provided improved surface coverage compared to raw CUR, CUR-F68 NS showed aggregation and incomplete coverage of the epithelium (C.V. = 0.99 ± 0.06, coverage = 70 ± 7%), suggesting that the insufficient surface coating by F68 compromised the mucosal distribution of the NS.[4a] In contrast, CUR-F127 NS provided highly uniform and near complete CUR distribution across the entire epithelial surface (C.V. = 0.49 ± 0.02, coverage = 91 ± 5%). It is notable that in airways treated with the NS formulations, a significant amount of drug fluorescence was found associated with the epithelial tissue, which is likely due to the enhanced dissolution of the NS (Figure 4a). In contrast, fluorescence from raw CUR was isolated to the aggregates in the airway lumen. It is possible that drugs within the epithelial layer may penetrate deeper into the underlying tissue via transcellular or paracellular mechanisms over a prolonged duration.[1a;28] The muco-inert coating of the NS likely further increases drug absorption by the tissue, as the coating prevents agglomeration in mucus, which would negatively impact the dissolution profile of the NS.[29]

Finally, we investigated whether the approach developed here would be applicable to NS composed of other hydrophobic therapeutics. We formulated F127-coated NS consisting of meso-tetra-(4-hydroxyphenyl) porphyrin (p-THPP), an investigative photo-sensitizer for photodynamic therapy.[30] Similar to CUR, p-THPP is water insoluble and possesses intrinsic fluorescence.[31] p-THPP-F127 NS displayed crystalline stability and shear-induced irregular morphology similar to those of CUR-F127 NS (Figure S6a,b). While the average size of p-THPP-F127 NS was larger than CUR-F127 NS (mean diameter = 323 nm, Table 1), their mobility in human CVM was comparable to that of CUR-F127 NS, with <MSD> at a time scale of 1s only 5-fold slower than the theoretical diffusion rates of similarly size nanoparticles in water (Table 1). Furthermore, p-THPP-F127 NS demonstrated enhanced dissolution rates compared to raw p-THPP (Figure S6c), and uniform distribution in the mouse airways following inhalation (Figure S6d). These results imply that our approach for developing muco-inert drug NS can be applied to other water insoluble drugs that form NS in aqueous solutions.

In summary, we developed mucus-penetrating NS composed of model poorly water soluble drugs, namely CUR and p-THPP, and coated with select Pluronics, in particular F127, which formed a muco-inert coating on the drug particulate surfaces. We showed that the coating efficiency by various materials was impacted by the MW of the hydrophobic segments of the surfactants and, therefore, their ability to coat the hydrophobic surfaces of the NS. The crystalline states of the drugs were maintained in the NS formulations, but their dissolution rates were greatly increased. In the mouse airways, mucus-penetrating NS provided improved mucosal distribution and appeared to enhance drug absorption by the epithelial tissues. Moreover, the all GRAS composition of mucus-penetrating NS and the success of existing NS-based clinical products should accelerate the translational development of the NS platform. Mucus-penetrating NS have great potential for treatment of diseases at mucosal surfaces, and potentially other tissues with similarly obstructive biological barriers, including brain tissues and peritoneal fluids.[26]

Supplementary Material

Refer to Web version on PubMed Central for supplementary material.

Acknowledgments

We thank Dr. Tyler M. McQueen and Ms. Kathryn Arpino for providing XRD facility and assistance with the XRD measurements. We also thank Dr. Ying-Ying Wang for critical review of the manuscript, Bruce Lim for helping with experiments, and Dr. Qingguo Xu, Dr. Ming Yang, and Dr. Benjamin Schuster for helpful discussions. This work is supported by the National Institute of Health (R01EB015031, U54CA151838, R01HD062844, and P01HL051811) and the Cystic Fibrosis Foundation (HANES07XX0).

References

1. a) Laffleur F, Bernkop-Schnurch A. Nanomedicine (Lond). 2013; 8:2061. [PubMed: 24279493] b) Kammona O, Kiparissides C. J Control Release. 2012; 161:781. [PubMed: 22659331]
2. a) Cone RA. Advanced drug delivery reviews. 2009; 61:75. [PubMed: 19135107] b) Thornton DJ, Sheehan JK. Proceedings of the American Thoracic Society. 2004; 1:54. [PubMed: 16113413] c) Lichtenberger LM. Annual review of physiology. 1995; 57:565.d) Lieleg O, Vladescu I, Ribbeck K. Biophysical journal. 2010; 98:1782. [PubMed: 20441741]
3. Lai SK, Wang YY, Hanes J. Advanced drug delivery reviews. 2009; 61:158. [PubMed: 19133304]
4. a) Wang YY, Lai SK, Suk JS, Pace A, Cone R, Hanes J. Angewandte Chemie International Ed In English. 2008; 47:9726. [PubMed: 18979480] b) Yang M, Lai SK, Wang YY, Zhong W, Happe C, Zhang M, Fu J, Hanes J. Angewandte Chemie International Ed In English. 2011; 50:2597. [PubMed: 21370345] c) Yu T, Wang YY, Yang M, Schneider C, Zhong W, Pulicare S, Choi WJ, Mert O, Fu J, Lai SK, Hanes J. Drug delivery and translational research. 2012; 2d) Xu Q, Boylan NJ, Cai S, Miao B, Patel H, Hanes J. J Control Release. 2013; 170:279. [PubMed: 23751567] e) Tang BC, Dawson M, Lai SK, Wang YY, Suk JS, Yang M, Zeitlin P, Boyle MP, Fu J, Hanes J. Proceedings of the National Academy of Sciences of the United States of America. 2009; 106:19268. [PubMed: 19901335] f) Kim AJ, Boylan NJ, Suk JS, Hwangbo M, Yu T, Schuster BS, Cebotaru L, Lesniak WG, Oh JS, Adstamongkonkul P, Choi AY, Kannan RM, Hanes J. Angewandte Chemie International Ed In English. 2013; 52:3985. [PubMed: 23460577]
5. Ensign LM, Tang BC, Wang YY, Tse TA, Hoen T, Cone R, Hanes J. Science translational medicine. 2012; 4:138ra79.
6. Yang M, Yu T, Wang YY, Lai SK, Zeng Q, Miao B, Tang BC, Simons BW, Ensign LM, Liu G, Chan KW, Juang CY, Mert O, Wood J, Fu J, McMahon MT, Wu TC, Hung CF, Hanes J. Adv Healthc Mater. 2014; 3:1044. [PubMed: 24339398]
7. Suk JS, Kim AJ, Trehan K, Schneider CS, Cebotaru L, Woodward OM, Boylan NJ, Boyle MP, Lai SK, Guggino WB, Hanes J. J Control Release. 2014; 178:8. [PubMed: 24440664]
8. Rabinow BE. Nature reviews. Drug discovery. 2004; 3:785. [PubMed: 15340388]
9. a) Suman J. Drug delivery and translational research. 2013; 3:4. [PubMed: 25787863] b) Davies NM. Clinical and experimental pharmacology & physiology. 2000; 27:558. [PubMed: 10874518]
10. Muller RH, Jacobs C, Kayser O. Advanced drug delivery reviews. 2001; 47:3. [PubMed: 11251242]
11. Bussemer T, Otto I, Bodmeier R. Critical reviews in therapeutic drug carrier systems. 2001; 18:433. [PubMed: 11763497]
12. Shegokar R, Muller RH. International journal of pharmaceutics. 2010; 399:129. [PubMed: 20674732]
13. Gao L, Liu G, Ma J, Wang X, Zhou L, Li X. J Control Release. 2012; 160:418. [PubMed: 22465393]
14. a) Kabanov AV, Batrakova EV, Alakhov VY. J Control Release. 2002; 82:189. [PubMed: 12175737] b) Kabanov AV, Lemieux P, Vinogradov S, Alakhov V. Advanced drug delivery reviews. 2002; 54:223. [PubMed: 11897147]
15. a) Aggarwal BB, Kumar A, Bharti AC. Anticancer research. 2003; 23:363. [PubMed: 12680238] b) Maheshwari RK, Singh AK, Gaddipati J, Srimal RC. Life sciences. 2006; 78:2081. [PubMed: 16413584]
16. Anand P, Kunnumakkara AB, Newman RA, Aggarwal BB. Molecular pharmaceutics. 2007; 4:807. [PubMed: 17999464]
17. Chignell CF, Bilski P, Reszka KJ, Motten AG, Sik RH, Dahl TA. Photochemistry and photobiology. 1994; 59:295. [PubMed: 8016208]
18. a) Singh R, Tonnesen HH, Kristensen S, Berg K. Photochemical & photobiological sciences : Official journal of the European Photochemistry Association and the European Society for Photobiology. 2013; 12:559.b) Sahu A, Kasoju N, Goswami P, Bora U. Journal of biomaterials applications. 2011; 25:619. [PubMed: 20207782]
19. Van Eerdenbrugh B, Van den Mooter G, Augustijns P. International journal of pharmaceutics. 2008; 364:64. [PubMed: 18721869]

20. a) Lai SK, Wang YY, Hida K, Cone R, Hanes J. Proceedings of the National Academy of Sciences of the United States of America. 2010; 107:598. [PubMed: 20018745] b) Suk JS, Lai SK, Wang YY, Ensign LM, Zeitlin PL, Boyle MP, Hanes J. Biomaterials. 2009; 30:2591. [PubMed: 19176245] c) Lai SK, Suk JS, Pace A, Wang YY, Yang M, Mert O, Chen J, Kim J, Hanes J. Biomaterials. 2011; 32:6285. [PubMed: 21665271] d) Schuster BS, Suk JS, Woodworth GF, Hanes J. Biomaterials. 2013; 34:3439. [PubMed: 23384790]
21. a) Lai SK, O'Hanlon DE, Harrold S, Man ST, Wang YY, Cone R, Hanes J. Proceedings of the National Academy of Sciences of the United States of America. 2007; 104:1482. [PubMed: 17244708] b) Suk JS, Lai SK, Boylan NJ, Dawson MR, Boyle MP, Hanes J. Nanomedicine (Lond). 2011; 6:365. [PubMed: 21385138]
22. Ensign LM, Cone R, Hanes J. Advanced drug delivery reviews. 2012; 64:557. [PubMed: 22212900]
23. Kocbek P, Baumgartner S, Kristl J. International journal of pharmaceutics. 2006; 312:179. [PubMed: 16469459]
24. Perry JL, Reuter KG, Kai MP, Herlihy KP, Jones SW, Luft JC, Napier M, Bear JE, DeSimone JM. Nano letters. 2012; 12:5304. [PubMed: 22920324]
25. Mert O, Lai SK, Ensign L, Yang M, Wang YY, Wood J, Hanes J. J Control Release. 2012; 157:455. [PubMed: 21911015]
26. a) Nance EA, Woodworth GF, Sailor KA, Shih TY, Xu Q, Swaminathan G, Xiang D, Eberhart C, Hanes J. Science translational medicine. 2012; 4:149ra119.b) Yang M, Yu T, Wood J, Wang YY, Tang B, Zeng Q, Simons B, Fu J, Chuang CM, Lai S, Wu TC, Hung CF, Hanes J. Drug delivery and translational research. 2014:1. [PubMed: 25786612]
27. a) Tay CY, Setyawati MI, Xie JP, Parak WJ, Leong DT. Advanced functional materials. 2014; 24:5936.b) Setyawati MI, Tay CY, Docter D, Stauber RH, Leong DT. Chemical Society reviews. 2015; 44:8174. [PubMed: 26239875]
28. a) Song Y, Wang Y, Thakur R, Meidan VM, Michniak B. Critical reviews in therapeutic drug carrier systems. 2004; 21:195. [PubMed: 15248809] b) Csaba N, Garcia-Fuentes M, Alonso MJ. Expert opinion on drug delivery. 2006; 3:463. [PubMed: 16822222]
29. Kesisoglou F, Panmai S, Wu Y. Advanced drug delivery reviews. 2007; 59:631. [PubMed: 17601629]
30. Berenbaum MC, Akande SL, Bonnett R, Kaur H, Ioannou S, White RD, Winfield UJ. British journal of cancer. 1986; 54:717. [PubMed: 2948536]
31. Bonnett R, McGarvey DJ, Harriman A, Land EJ, Truscott TG, Winfield UJ. Photochemistry and photobiology. 1988; 48:271. [PubMed: 3222336]

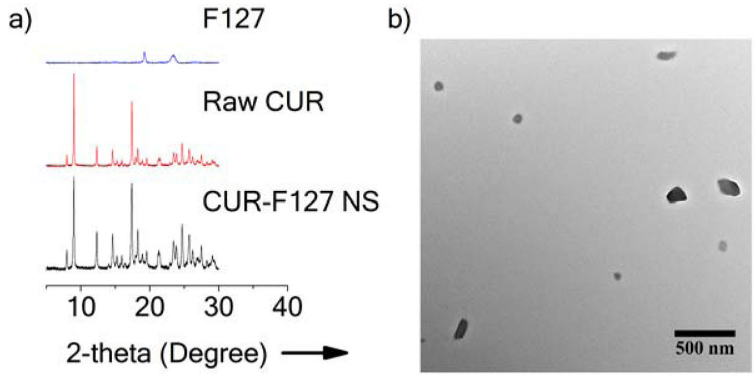

Figure 1.

Physical characterization of CUR-F127 NS. a) Powder X-ray diffraction (Powder-XRD) diagram of F127, raw curcumin (Raw CUR) and CUR-F127 NS. b) Representative TEM image of CUR-F127 NS.

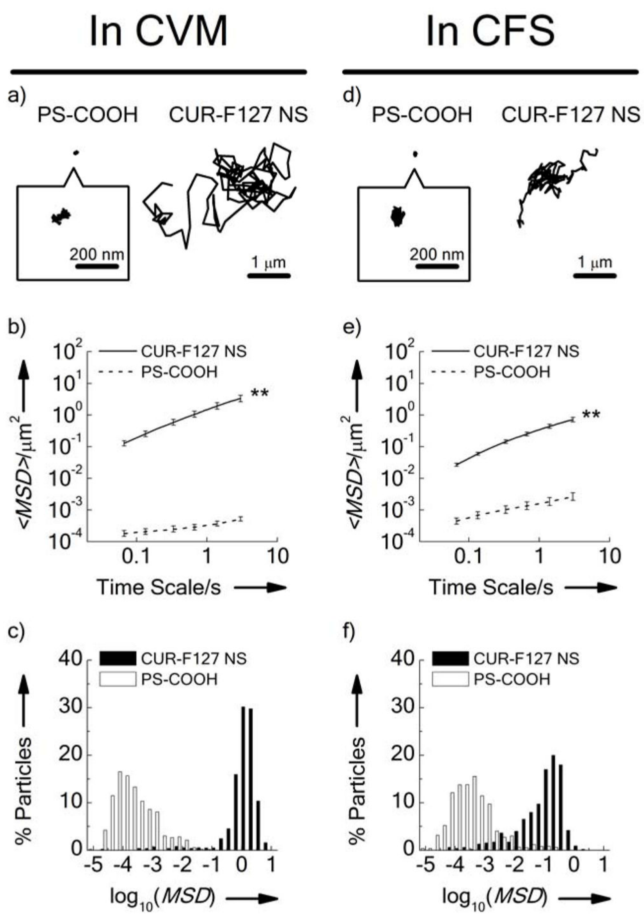

Figure 2.

Transport behavior of uncoated PS-COOH nanoparticles and CUR-F127 NS in a–c) human cervicovaginal mucus (CVM) (Left) and d–f) cystic fibrosis sputum (CFS) (Right). a&d) Representative trajectories of PS-COOH nanoparticles and CUR-F127 NS. b&e) Ensemble averaged geometric mean-squared displacements (<MSD>) as a function of time scale. c&f) Distributions of the logarithms of individual particle MSD at a time scale of 1 s. Data represent the ensemble average of five independent experiments, with n ≥ 100 particles tracked for each experiment. Error bars indicate geometric standard error. (**, p<0.01 for all time scales analyzed).

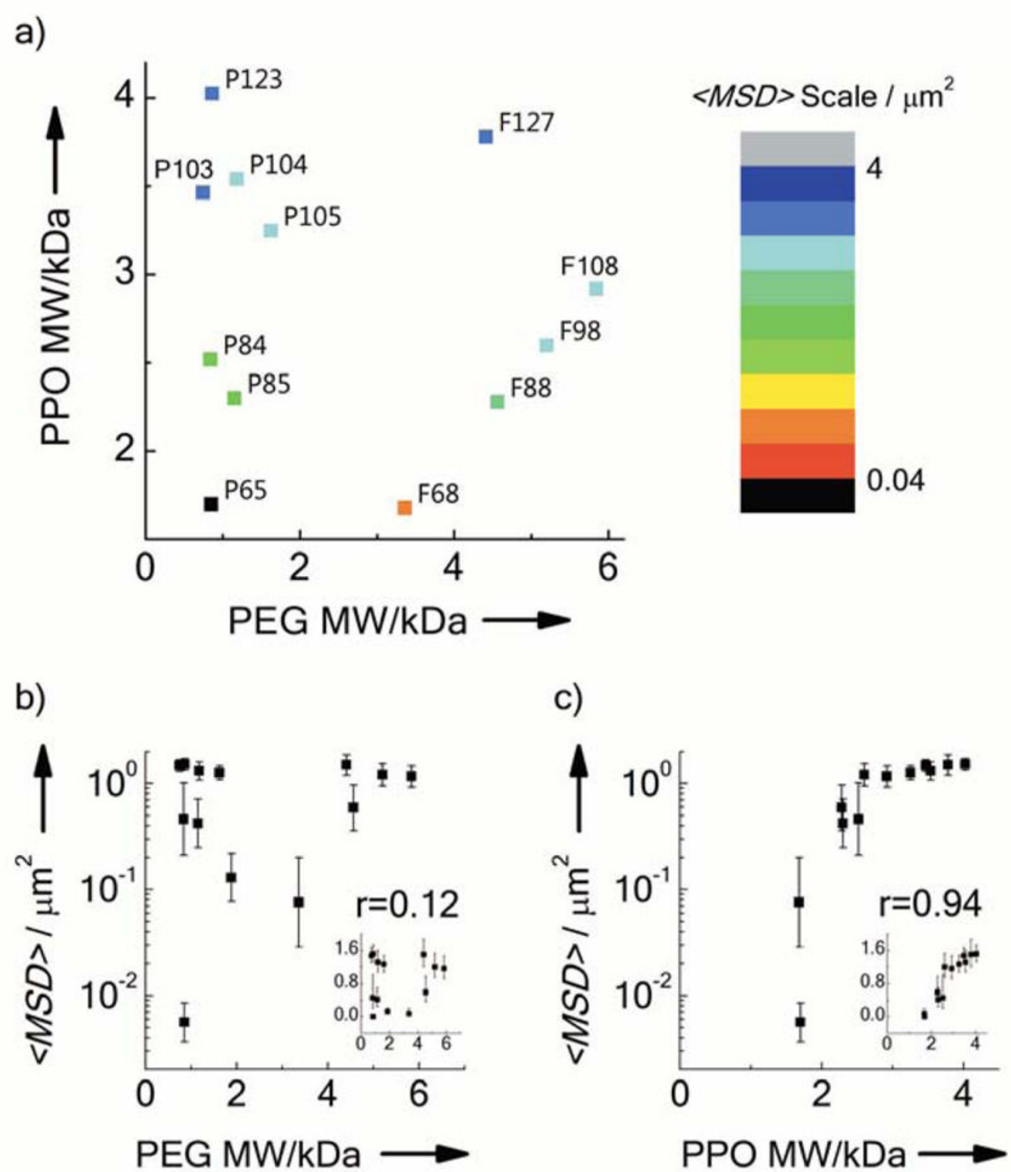

Figure 3.

Mobility of CUR NS formulated with different Pluronics coatings in human CVM. a) Phase diagram correlating <MSD> at a time scale of 1s of CUR NS to the MW of the Pluronics PEG segments and the poly(propylene oxide) (PPO) segment. Each data point represents a specific type of Pluronic, as indicated. b–c) <MSD> at a time scale of 1 s as a function of the MW of b) PEG or c) PPO segments. The insets represent the same plot with linear scale of <MSD>, while r represents the correlation coefficient. Data represent the ensemble average of at least three independent experiments, with n ≥ 100 particles tracked for each experiment. Error bars indicate geometric standard error.

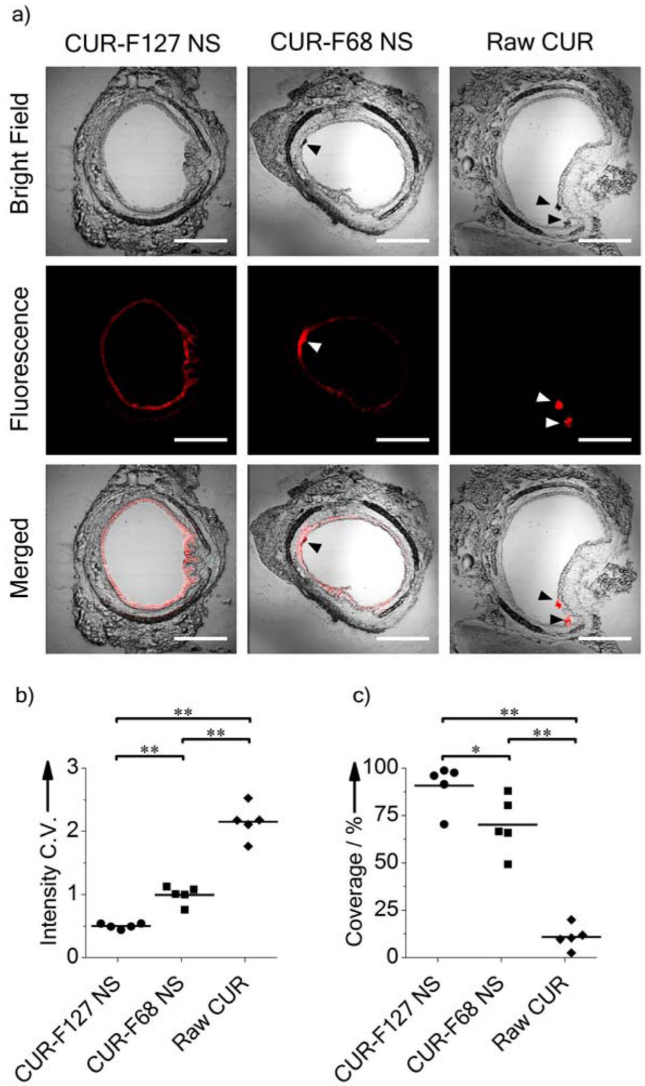

Figure 4.

Distribution of CUR-F127 NS, CUR-F68 NS and Raw CUR in mouse airways. a) Transverse frozen sections of mouse trachea tissue following intranasal administration of NS or raw drug suspension. Red represents CUR fluorescence. Arrows indicate drug aggregates. Scale bars represent 500 μm. b) Coefficient of variations (C.V.) of fluorescence intensity profiles along the airway epithelial surface. Lower C.V. represents better uniformity of distribution. c) Percent coverage of CUR along the airway epithelial surface. (*, $p < 0.05$; **, $p < 0.01$; n = 5 mice for each group.)

Table 1

Size and ζ-potential of F127 and F68-coated NS formulations and uncoated PS-COOH nanoparticles with ratios of their ensemble average MSD in human CVM ($\langle MSD \rangle_m$) compared to the theoretical diffusion rates in water (MSD_w).

NS/Particle Type	Mean Diameter [nm][a]	ζ-Potential [mV][a]	$MSD_w/\langle MSD \rangle_m$ [b]	
			in CVM	in CFS
CUR-F127	133 ± 12	− 0.8 ± 0.1	9	37
CUR-0.1%F127	154 ± 4	− 1.4 ± 0.4	11	–
CUR-0.01%F127	176 ± 11	− 1.6 ± 0.3	35	–
CUR-0.001%F127	184 ± 30	− 1.3 ± 0.5	10,000	–
CUR-F68	154 ± 20	− 1.4 ± 0.1	150	–
p-THPP-F127	323 ± 8	0.3 ± 0.4	5	–
PS-COOH	210 ± 15	− 50 ± 4	25,000	5,200

[a]Mean diameter and ζ-potential were measured via dynamic light scattering and laser Doppler electrophoresis, respectively. Data represent mean ± standard error (n ≥ 3).

[b]MSD_w is calculated from the Stokes-Einstein equation based on average particle diameter and at the time scale of 1s. $\langle MSD \rangle_m$ is the geometric ensemble average of MSD at a time scale of 1s.